SMC-TR-94-40

AEROSPACE REPORT NO.
TR-94(4911)-1

# Threshold Detection in the Presence of Atmospheric Turbulence

15 October 1994



Prepared by

H. T. YURA
Electronics Technology Center
Technology Operations

Prepared for

SPACE AND MISSILE SYSTEMS CENTER
AIR FORCE MATERIEL COMMAND
2430 E. El Segundo Boulevard
Los Angeles Air Force Base, CA 90245



Development Group

This report was submitted by The Aerospace Corporation, El Segundo, CA 90245-4691, under Contract No. F04701-93-C-0094 with the Space and Missile Systems Center, 2430 E. El Segundo Blvd., Los Angeles Air Force Base, CA 90245. It was reviewed and approved for The Aerospace Corporation by T. Galantowicz, Principal Director, Electronics Technology Center.

This report has been reviewed by the Public Affairs Office (PAS) and is releasable to the National Technical Information Service (NTIS). At NTIS, it will be available to the general public, including foreign nationals.

This technical report has been reviewed and is approved for publication. Publication of this report does not constitute Air Force approval of the report's findings or conclusions. It is published only for the exchange and stimulation of ideas.

William E. Slutter, Capt. USAF
MSTRS Program Manager
SMC/XRX

# REPORT DOCUMENTATION PAGE

*Form Approved*
*OMB No. 0704-0188*



| 1 AGENCY USE ONLY (*Leave blank*) | 2 REPORT DATE | 3 REPORT TYPE AND DATES COVERED |
|---|---|---|
| | 15 October 1994 | |

**4 TITLE AND SUBTITLE**
Threshold Detection in the Presence of Atmospheric Turbulence

**5 FUNDING NUMBERS**
F04701-93-C-0094

**6 AUTHOR(S)**
H. T. Yura

**7 PERFORMING ORGANIZATION NAME(S) AND ADDRESS(ES)**
The Aerospace Corporation
P. O. Box 92957
Los Angeles, CA 90009-2957

**8 PERFORMING ORGANIZATION REPORT NUMBER**
TR-94(4911)-1

**9 SPONSORING/MONITORING AGENCY NAME(S) AND ADDRESS(ES)**
Space and Missile Systems Center
Air Force Materiel Command
2430 E. El Segundo Boulevard
Los Angeles Air Force Base, CA 90245

**10 SPONSORING/MONITORING AGENCY REPORT NUMBER**
SMC-TR-94-40

**11 SUPPLEMENTARY NOTES**

**12a DISTRIBUTION/AVAILABILITY STATEMENT**
Approved for public release; distribution unlimited

**12b DISTRIBUTION CODE**

**13 ABSTRACT** (*Maximum 200 words*)

Recently, there has been increased interest in threats to spacecraft from ground-based lasers. It has been suggested that some spacecraft should employ laser-threat warning receivers. Here, we consider the effects of atmospheric turbulence on threshold detection of optical signals by an exoatmospheric receiver. The present results are applicable to both cw and pulsed optical illumination from ground-based lasers. In particular, we obtain accurate analytical expressions, over a wide range of conditions of practical interest, that give the required signal-to-noise ratio for a given (single-event) probability of detection, false-alarm rate, and turbulence-induced log-intensity variance. The degrading effects of atmospheric turbulence on threshold detection are most important for large zenith angles in the blue-green region of the spectrum. As an illustrative example, a false-alarm rate of one in three years is assumed, and specific numerical results are presented for the required signal-to-noise ratio necessary to obtain a detection probability of at least 95% over a range of optical wavelengths and propagation conditions of interest.

| 14 SUBJECT TERMS | 15. NUMBER OF PAGES |
|---|---|
| Threshold detection, Atmospheric turbulence, Scintillation | 15 |
| | 16. PRICE CODE |

| 17 SECURITY CLASSIFICATION OF REPORT | 18 SECURITY CLASSIFICATION OF THIS PAGE | 19 SECURITY CLASSIFICATION OF ABSTRACT | 20. LIMITATION OF ABSTRACT |
|---|---|---|---|
| UNCLASSIFIED | UNCLASSIFIED | UNCLASSIFIED | |

# Preface

I wish to thank J. H. Churnside of NOAA/ETL, Boulder, CO., for his helpful comments and critical reading of the manuscript.

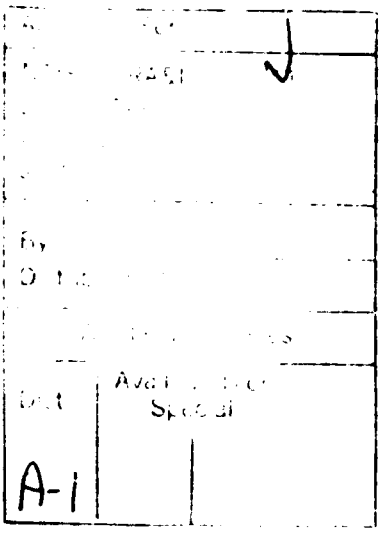

## Contents



## Figures



## Table

# 1. Introduction

Ground-based lasers have been used increasingly to illuminate satellites in space. These lasers can be used to track the satellites and to temporarily or permanently impair their intended performance. It is highly desirable that the threat to system performance posed by such ground-based lasers be mitigated. In order to mitigate this threat, the ground-based laser illumination must be detected and characterized at low enough fluence levels that no harm results to sensitive subsystem components. Upon detection, measures can then be employed to protect the integrity of the spacecraft and its subsystems. However, a large false-alarm rate (FAR) would interfere undesirably with normal satellite operations. Thus, a requirement for any viable laser warning threat reporting system will be that it has a large single-event probability of detection (e.g., $\geq$ 95%) and a very low FAR (e.g., one in three years). Additionally, it is desirable to detect both cw and pulsed lasers sources over a wide spectral range (e.g., 0.4–14 μm). In this report, we derive expressions for both the threshold-to-noise ratio (TNR) and signal-to-noise ratio (*SNR*) that are independent of the specific system design of the laser threat-reporting receiver. These expressions are derived for the performance of the system in the presence of atmospheric turbulence for given values of both the probability of detection and FAR over a wide range of practical interest.

In this regard, we consider an exoatmospheric-based, direct-detection receiver system that employs a threshold-detection algorithm to determine the presence of optical illumination that results from a ground-based laser source. This determination is obtained from the observation of a suitable photodetector current (or voltage) over a measurement sample time determined by the reciprocal of the bandwidth of the receiver. In particular, the detector photocurrent is measured over the sample time and presented to a threshold circuit. When the photocurrent exceeds a predetermined threshold, the decision is made that an illuminating signal is present; when the photocurrent fails to exceed the threshold, the decision is made that no signal is present.

In this paper, we consider both pulsed and cw illumination and derive expressions for the probability of detection in the presence of atmospheric turbulence. Previously, atmospheric turbulence effects on threshold detection have been considered by Teich and Rosenberg[1], and Churnside and McIntyre.[2] However, in contrast to the present analysis, only the very low signal level in the photon-counting regime was considered. Here, we assume that the mean photo count is large, and, thus, Gaussian statistics are applicable. In Sec. 2, we briefly review system noise degradations and present an expression for the TNR as a function of the FAR. In Sec. 3, we present results for the detection probability as a function of both the threshold- and signal-to-noise ratio. Then, in Sec. 3, we include the effects of atmospheric turbulence on system performance. As is discussed in Sec. 3, atmospheric turbulence-induced scintillation of the illuminating laser beam (i.e., irregular intensity fluctuations) will reduce receiver performance in comparison to a constant signal with the same average intensity. In particular, for a given FAR and the variance of the atmospheric turbulence-induced intensity fluctuations, we derive an expression for the probability of detection as a function of the SNR. By inverting this relationship, we obtain accurate numerical expressions that give the required SNR for a given (single-event) probability of detection, FAR, and turbulence-induced log-intensity variance. As such, these accurate analytic approximations for the SNR in the presence of atmospheric turbulence will be useful in aiding

the system analyst in parametric estimation of system performance under various operational conditions.

Specific numerical results are then illustrated for a $FAR/f = 10^{-11}$, where $f$ = low-pass receiver filter bandwidth, and a detection probability of 95% for various optical wavelengths and propagation conditions. A $FAR/f$ of $10^{-11}$ corresponds to a false-alarm rate of about one in three years for a 1-kHz lowpass receiver bandwidth. The results obtained here for system performance are expressed in terms of dimensionless ratios of both the signal- and threshold-to-noise. As such, the results presented here are independent of the specific design details of the system and are applicable to a general threshold detection receiver system. For a specific proposed operational system, absolute numerical values of the relevant parameters can then be obtained (e.g., required incident fluence for a given level of performance).

## 2. Noise

The receiver system has to be designed to operate in the presence of the various noise contaminations that can produce false alarms (i.e., detection decisions when the signal is not present). In general, when no signal is present, receiver noise sources include background shot noise, receiver dark current, and thermal noise. Following Kingston,[3] we assume, in the absence of turbulence, that both noise and signal photocurrent statistics can be adequately modeled by Gaussian statistics.[4] Rice[5] has derived the relationship between the TNR and the FAR. His results can be expressed as

$$TNR = \sqrt{-2\ln\left(\sqrt{3}FAR/f\right)}, \tag{2.1}$$

where *ln* denotes the natural logarithm,

$$TNR = \frac{i_t}{\sigma_n}, \tag{2.2}$$

$i_t$ is the threshold current, and $\sigma_n$ is the standard deviation of the noise photocurrent (i.e., the non-signal-related noise).

Figure 1 is a plot of the TNR as a function of $FAR/f$ over a range of interest. For example, for $FAR/f = 10^{-11}$ we obtain that the required $TNR = 7.04$. That is, in order for a threshold detection system to operate at a $FAR/f$ of $10^{-11}$ a TNR of about 7.0 is required, independent of the details of the receiver design. For a given receiver design and operational scenario (i.e., detector characteristics, field-of-view, collecting aperture area, bandwidth, background noise spectral radiance, etc.), one can then obtain a numerical value for $\sigma_n$, and for a given $FAR/f$, an explicit value for $i_t$ can then be obtained from Eq. (2.2).

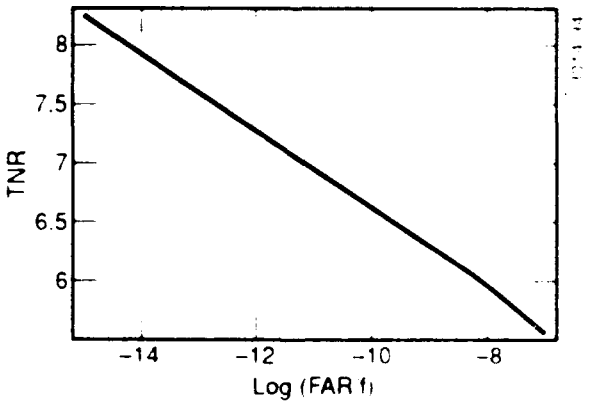


Figure 1. The threshold-to-noise ratio as a function of the false-alarm rate.

## 3. Threshold Detection in the Absence of Turbulence

First, we review the salient features of threshold detection in the absence of turbulence, where a constant signal is present. Because both the signal and noise photocurrents are Gaussian variates (see Ref. 3), the probability distribution of signal plus noise is also Gaussian, with the mean equal to the mean signal photocurrent, $i_S$, and a standard deviation, $\sigma_{Sn}$, given by

$$\sigma_{Sn} = \sqrt{\sigma_S^2 + \sigma_n^2}\,, \tag{3.1}$$

where $\sigma_S$ is the standard deviation of the signal shot noise. The probability of detection, $p_d$, is obtained by integrating the probability of signal plus noise above the threshold current, $i_t$. The result is given by

$$p_d = \frac{1}{2}\left(1 + erf\left[\frac{i_S - i_t}{\sqrt{2}\sigma_{Sn}}\right]\right), \tag{3.2}$$

where $erf(\cdot)$ denotes the error function.

Here, we neglect signal shot noise with respect to other noise sources (e.g., background-induced shot noise) and hence, in what follows, we assume that $\sigma_{Sn} = \sigma_n$.[6] Hence, the probability of detection can be expressed as

$$p_d = \frac{1}{2}\left(1 + erf\left[\frac{SNR - TNR}{\sqrt{2}}\right]\right), \tag{3.3}$$

where the $SNR$ is given by

$$SNR = \frac{i_S}{\sigma_n}. \tag{3.4}$$

Figure 2 is a plot of the required SNR in the absence of turbulence versus $FAR/f$ for various values of the detection probability. For the values of $p_d$ shown in Figure 2, an analytic expression for the SNR in the absence of turbulence, $SNR_O$, is given by

$$\begin{aligned} SNR_O &= TNR + \delta \\ &= \sqrt{-2\ln\left(\sqrt{3}FAR/f\right)} + \delta, \end{aligned} \tag{3.5}$$

where $\delta$ = 1.64, 2.33, 3.09, 3.72, for $p_d$ = 95%, 99%, 99.9%, and 99.99%, respectively. An accurate analytical approximation for $\delta$, based on the asymptotic expansion of the error function in Eq. (3.3) for large values of its argument, is given by

$$\delta = \sqrt{2}\left(\delta_o - \frac{\ln\left[\delta_o\left(1+1/2\delta_o^2\right)\left(1-\ln\delta_o/2\delta_o^2\right)\right]}{2\delta_o}\right), \tag{3.6}$$

where

$$\delta_o = \sqrt{-\ln\left[2\sqrt{\pi}\left(1-p_d\right)\right]}. \tag{3.7}$$

The accuracy of Eq. (3.6) is better than about 1.2% for $0.95 \le p_d \le 1$. For example, for $FAR/f = 10^{-11}$ examination of Figure 2 [or, as indicated by Eq. (3.5)] reveals that a 95% and 99% probability of detection is obtained for a $SNR$ = 8.68, and 9.37, respectively, independent of the details of receiver design.

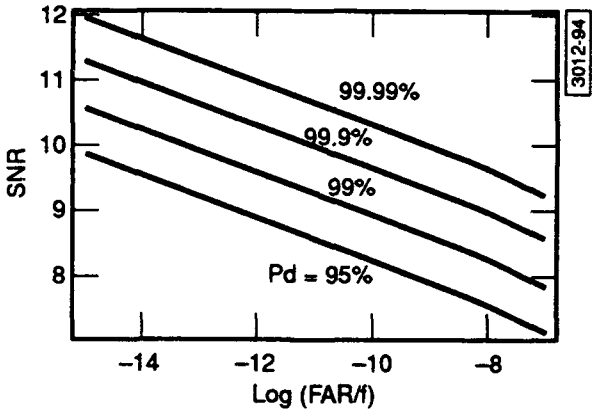


Figure 2. The signal-to-noise ratio in the absence of turbulence as a function of $FAR/f$ for various values of the probability of detection.

## 4. Threshold Detection in the Presence of Turbulence

When a small photodetector is placed in the path of a laser beam propagating through the atmosphere, irregular fluctuations of intensity are readily observed with a scintillation bandwidth of a few tenths to a few hundred hertz.[7] Here, we are concerned with propagation up through the atmosphere from a ground-based laser source. In order to be as conservative as possible, we assume that the observed scintillation characteristics are given by that for a ground-based point source since finite-beam wave scintillation effects are less than the corresponding point-source effects.[8]

Experimental results of nighttime scintillation measurements at a satellite from a ground-based laser transmitter have been reported by Minott.[9] A detector aboard the GEOS-11 satellite at an altitude of 1250 km was illuminated by a 0.488 μm cw argon laser. Log-amplitude variance, probability distributions, and scintillation frequency distributions were derived from the data. It was concluded that, within the experimental errors, the observed results were in agreement with theoretical predictions given in the literature.[7] In particular, as predicted by theory, the intensity probability distribution was shown to be log-normal, and the observed log-amplitude variances were shown to be in the limits measured for ground-based stellar observations for zenith angles less than about 60°. Typical scintillation bandwidths were observed to be in the range of about 90–180 Hz, in agreement with predictions. In addition, the scintillation correlation length for an exoatmospheric observer can be assumed to be much larger than tens of meters for all optical wavelengths and propagation paths of interest.[10] As such, no aperture averaging effects are expected to be obtained at the receiver.

Atmospheric turbulence-induced scintillation will affect the performance of a threshold detector when the fluctuation rate of the incident intensity is small compared to the measurement sample time, $\tau$ (i.e., over a measurement interval $\tau$ the signal strength remains constant). Considering atmospheric winds, low earth-satellite motions, and up propagation through the atmosphere, it can be shown that this assumption is valid for $\tau \ll 10^{-2}$ s. Therefore, the analysis given below is seen to be applicable to both cw detection employing measurement sample times $\ll$ 10 ms and detection of short pulses (e.g., Q-switched laser pulses) with corresponding interpulse separations $\gg$ 10 ms. For detection of cw signals employing measurement sample times large compared with the scintillation characteristic time scale of 10 ms, temporal averaging will occur, and the results given in Sec. 2 for a constant signal apply. Additionally, because the averaging of a log-normal process produces a process that is very nearly log-normal (Central Limit theorem convergence is very slow for a log-normal process),[11] the results of this paper are also valid for partial temporal averaging (i.e., $\tau \sim 10$ ms), with a variance that is reduced by that averaging.[12] Temporal averaging can be expected to be obtained for cw illumination for $\tau > \tau_S$, where $\tau_S$ is the characteristic scintillation scale time, and for pulsed illumination for repetition rates $> \tau_S^{-1}$ (referred to here as quasi-cw illumination).

Because of the assumption of slow fading relative to the measurement sample time $\tau$, the signal photocurrent statistics during each sample time are Gaussian, and the expression for the probability of detection given in Sec. 2 applies, with $i_S$ replaced by the photocurrent, $i$, that corresponds

to the (fluctuating) intensity that is present during this sample time. Now, $i$ fluctuates from sample interval to sample interval, as does the short-term (i.e., over a sample interval) value of $p_d$. To obtain the long-term probability of detection, $p_d$ must be averaged over the fluctuation of $i$. Assuming that the atmospheric statistics are stationary (i.e., that the fluctuation statistics remain constant in time), the long-term average over the fluctuations in $i$ can be evaluated as an ensemble average and expressed in terms of the probability density function of $i$ [denoted by $p_i(i)$]. We have,

$$\langle p_d \rangle = \int_0^\infty p_d(i) p_i(i) di, \tag{4.1}$$

where angular brackets denote the ensemble average over the atmospheric turbulence statistics,

$$p_d(i) = \frac{1}{2}\left(1 + erf\left[\frac{i - i_t}{\sqrt{2}\sigma_n}\right]\right), \tag{4.2}$$

and, since $i$ is proportional to intensity, which is log-normally distributed,

$$p_i(i) = \frac{1}{\sqrt{2\pi\sigma_{\ln I}^2}} \frac{1}{i} \exp\left(-\frac{\left[\ln\left(i/\langle i_s \rangle\right) + \frac{1}{2}\sigma_{\ln I}^2\right]^2}{2\sigma_{\ln I}^2}\right), \tag{4.3}$$

where $\langle i_s \rangle$ is the ensemble averaged photocurrent, and $\sigma_{\ln I}^2$ is the log-intensity variance obtained over a measurement sample time, $\tau$. For weak scintillation conditions (i.e., $\sigma_{\ln I}^2 < 1$), it can be shown that an accurate engineering expression for $\sigma_{\ln I}^2$ can be expressed as[7,12]

$$\sigma_{\ln I}^2 = \begin{cases} 4\chi^2 & \text{(short pulse illumination)} \\ 4\chi^2\left(\dfrac{1}{1 + (\tau/\tau_s)^{7/6}}\right) & (cw \text{ and quasi-cw illumination}) \end{cases}, \tag{4.4}$$

where the log-amplitude variance, $\chi^2$, is given by[13]

$$\chi^2 = 0.56 k^{7/6} \mu_{5/6} \sec(Z)^{11/6}; \tag{4.5}$$

$k$ is the optical wave number (= $2\pi/\lambda$, where $\lambda$ is the wavelength), $Z$ is the zenith angle,

$$\mu_{5/6} = \int_0^\infty C_n^2(h) h^{5/6} dh, \tag{4.6}$$

and $C_n^2(h)$ is the index structure constant profile as a function of altitude $h$ above ground. The quantity in the brackets on the right-hand side of Eq. (4.4) is the cw weak scintillation temporal averaging (reduction) factor that gives the effects of the finite measurement sample time on the observed scintillation. As expected, for $\tau << \tau_s$, $\sigma^2_{\ln I} = 4\chi^2$, while for $\tau >> \tau_s$, $\sigma^2_{\ln I} = 0$. Examination of Eq. (4.5) reveals that the strength of scintillation, as measured by the log-amplitude variance, is proportional to $\lambda^{-}s(Z)^{11/6}$, and, hence, scintillation effects are most pronounced in the blue-green and at large zenith angles.

There are several $C_n^2(h)$ profiles that have been used extensively by the technical community for ground-to-space applications. Recently, these profiles have included the Hufnagel Valley 5/7 model,[14] the Clear1 model,[15] the Clear2 model,[16] and the Navy-DARPA SLC day model.[17]. Although they differ in detail, they all yield similar results for the integral $\mu_{5/6}$ given in Eq. (3.6). Specifically, we have: $\mu_{5/6} = 5.35 \times 10^{-10}\ m^{7/6}$ (Hufnagel Valley 5/7 model), $\mu_{5/6} = 3.70 \times 10^{-10}\ m^{7/6}$ (Clear1 model), $\mu_{5/6} = 5.11 \times 10^{-10}\ m^{7/6}$ (Clear2 model), and $\mu_{5/6} = 4.54 \times 10^{-10}\ m^{7/6}$ (Navy-DARPA SLC day model). In view of this, we employ here a nominal conservative value of $\mu_{5/6} = 5.0 \times 10^{-10}\ m^{7/6}$ in order to obtain numerical results. As a result, we obtain from Eq. (3.5) that

$$\chi^2 = 0.024 \lambda_{\mu m}^{-7/6} \sec(Z)^{11/6}, \tag{4.7}$$

where $\lambda_{\mu m}$ is the wavelength in microns.[18] From Eqs. (4.4) and (4.7), it is easily seen that weak scintillation conditions are obtained for zenith angles less than about 60–65° in the visible with larger zenith angles allowed for wavelengths in the infrared.

As an illustrative numerical example, we consider a $FAR/f = 10^{-11}$, short-pulsed or cw illumination for $\tau << \tau_s$ (i.e., $\sigma^2_{\ln I} = 4\chi^2$), a log-amplitude variance of 0.075 (e.g., $\lambda = 1$ μm, and Z = 57.5°) and plot in Figure 3 the (ensemble averaged) probability of detection as a function of the signal-to-noise ratio; SNR = $\langle i_s \rangle / \sigma_n$. Examination of Figure 3 reveals that in the presence of turbulence a SNR of about 20.6 is required in order to obtain a probability of detection of 95%. This is in contrast to the absence of turbulence, where we have seen in Sec. 2 that the corresponding SNR is about 8.7. This implies, assuming everything else to be equal, that it requires about 2.4 times more average signal strength to achieve a detection probability of 95% than would be obtained by neglecting atmospheric turbulence effects. Additionally, the SNR that yielded a 95% detection probability in the absence of turbulence (i.e., 8.7) yields now, in the presence of turbulence, a detection probability of only 55%.

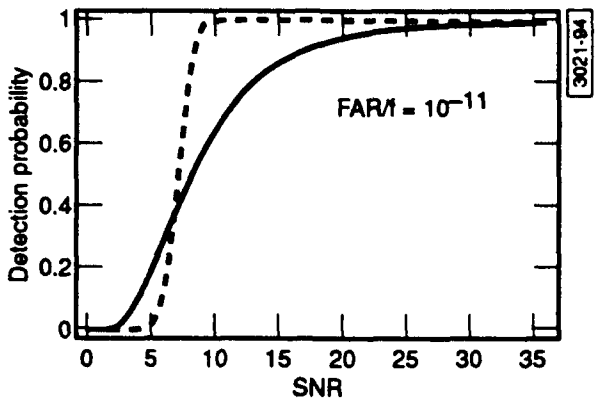


Figure 3. Detection probability versus the signal-to-noise ratio for a $FAR/f = 10^{-11}$. The dashed and solid curves refer to the absence of turbulence and a log-amplitude variance of 0.075, respectively. A $FAR/f = 10^{-11}$ corresponds to a FAR of about one in three years for a lowpass receiver bandwidth $f = 1$ kHz.

For the $p_d$ shown in Figure 2, an accurate analytic engineering approximation for the required SNR as a function of both $FAR/f$, and log-intensity variance is given by

$$SNR = SNR_0 + \Psi_1(FAR/f)\sigma^2_{\ln I} + \Psi_2(FAR/f)\sigma^4_{\ln I}, \tag{4.8}$$

where $SNR_0$ is given by Eq. (3.5), $\sigma^2_{\ln I}$ is given by Eq. (3.4),

$$\Psi_1(FAR/f) = a_1 + b_1 \log(FAR/f) + c_1[\log(FAR/f)]^2, \tag{4.9}$$

$$\Psi_2(FAR/f) = a_2 + b_2 \log(FAR/f) + c_2[\log(FAR/f)]^2, \tag{4.10}$$

and the coefficients $a_1, b_1, \ldots, c_2$ are listed in Table 1 for various values of $p_d$. Accurate numerical analytical approximations to these coefficients are given by

$$a_1(p_d) = -32.39 + 115.19x + 15.63\sqrt{-\ln(x)} - 3.36\ln(x), \tag{4.11}$$

$$b_1(p_d) = 3.77 + 6.66x - 4.7\sqrt{-\ln(x)} - 0.316\ln(x), \tag{4.12}$$

$$c_1(p_d) = -0.537 + 4.02x + 0.324\sqrt{-\ln(x)} + 0.06\ln(x), \tag{4.12}$$

$$a_2(p_d) = 248.16 - 264.52x - 236.89\sqrt{-\ln(x)} - 60.23\ln(x), \tag{4.13}$$

$$b_2(p_d) = -79.63 + 113.38x + 71.71\sqrt{-\ln(x)} + 16.7\ln(x), \tag{4.14}$$

$$c_2(p_d) = -1.96 + 3.17x + 1.69\sqrt{-\ln(x)} + 0.373\ln(x), \tag{4.15}$$

and

$$x = 1 - p_d. \tag{4.16}$$

The accuracies of Eqs. (4.8)–(4.16) are better than 1% over the range $10^{-15} \le FAR/f \le 10^{-7}$, $0.95 \le p_d \le 0.9999$, and $0 \le \sigma^2_{\ln I} \le 0.5$, which is of practical interest. Equations (4.8)–(4.16) were obtained by a least-squares fit to calculated values of the SNR over the range given above.

Note that Eq. (4.8) is based on the assumption of a log-normal probability distribution for the intensity fluctuations. Hence, as long as the turbulence-induced intensity fluctuations are log-normally distributed, Eq. (4.8) gives the required SNR as a function of the false-alarm rate and the log-intensity variance to obtain the indicated probability of detection. As an example, we plot in Figure 4 the SNR as a function of $\sigma^2_{\ln I}$ for a $FAR/f = 10^{-11}$ and various values of $p_d$.

We now consider short-pulsed or cw illumination for $\tau << \tau_s$ (i.e., $\sigma^2_{\ln I} = 4\chi^2$) and present specific numerical results for propagation up through the atmosphere. Figure 5 is a plot of the required SNR as function of zenith angle for $FAR/f = 10^{-11}$ and various wavelengths of interest. Similarly, we plot in Figure 6 the corresponding SNR versus wavelength for some representative values of zenith angle. Examination of these figures reveals that for wavelengths greater than about 3–4 μm, the effects of atmospheric turbulence on receiver performance are insignificant for zenith angles less than about 60°.

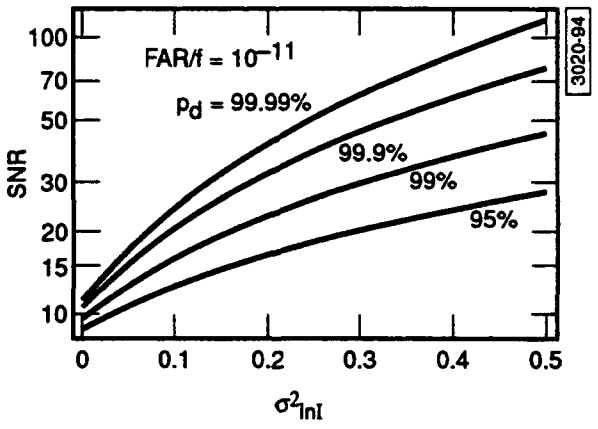


Figure 4. The signal-to-noise ratio as a function of the variance of log-intensity for a $FAR/f = 10^{-11}$ and various values of the probability of detection.

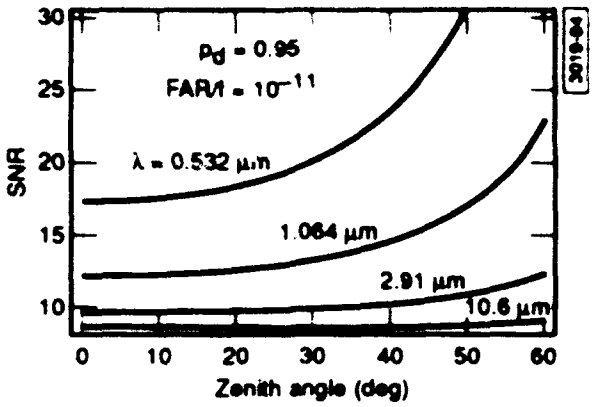


Figure 5. The signal-to-noise ratio as a function of the zenith angle for a detection probability of 95%, a $FAR/f = 10^{-11}$, and various wavelengths of interest.

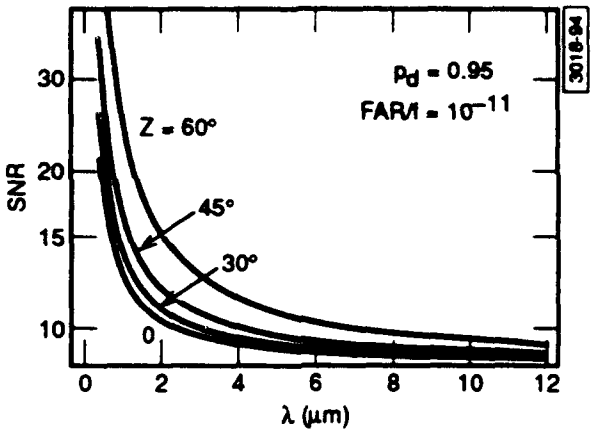


Figure 6. The signal-to-noise ratio as a function of wavelength for a detection probability of 95%, a $FAR/f = 10^{-11}$, and various zenith angles.

## 5. Conclusion

We have considered threshold detection in the presence of atmospheric turbulence. Based on the log-normal probability distribution for turbulence-induced intensity fluctuations, we have derived both numerical and analytic results, over a wide range of conditions of practical interest, for the SNR as a function of (the given) $p_d$, $FAR$, and $\sigma^2_{\ln I}$. The results presented here are applicable to both cw detection systems utilizing measurement sample times that are short compared to the atmospheric scintillation time scales and the detection of short pulses at repetition rates < 100 Hz. As such, these accurate analytical approximations for the SNR in the presence of atmospheric turbulence will be useful in aiding the system analyst in parametric estimation of system performance under various operational conditions. Specific numerical results are presented for laser propagation up through the atmosphere, where it is shown that the degrading effects of turbulence are most important for large zenith angles in the blue-green region of the spectrum.

Table 1. The coefficients appearing in Eqs. (4.9) and (4.10) for various values of the probability of detection.

| $p_d$(%) | $a_1$ | $b_1$ | $c_1$ | $a_2$ | $b_2$ | $c_2$ |
|---|---|---|---|---|---|---|
| 95 | 10.49 | -3.09 | -0.0461 | 5.35 | 0.407 | 0.001 |
| 99 | 17.78 | -4.08 | -0.0759 | 14.52 | -1.23 | -0.0265 |
| 99.9 | 32.02 | -6.40 | -0.0929 | 41.34 | -6.11 | -0.1 |
| 99.99 | 46.01 | -7.59 | -0.0461 | 83.93 | -15.5 | -0.276 |

## References and Notes


[1]M. C. Teich and S. Rosenberg, Photocounting array receivers for optical communication through the log-normal atmospheric channel. 1: Optimum and suboptimum receiver structures, Appl. Opt. **12**, 2616-2624, (1973). S, Rosenberg and M. C. Teich, Photocounting array receivers for optical communication through the log-normal atmospheric channel. 2: Optimum and suboptimum receiver performance for binary signaling, Appl. Opt. **12**, 2625-2635, (1973).

[2]J. H. Churnside, Averaged threshold receiver for direct detection of optical communication through the log-normal atmospheric channel, Appl. Opt. **16**, 2669-2676, (1977).

[3] R. H. Kingston, Detection of Optical and Infrared Radiation, Springer Verlag Publishing Co., New York, 1979. In this regard, also see The Infrared and Electrooptical Systems Handbook, Vol. 7, D. H. Pollock, Ed., Chap. 1, Pub. by ERIM/SPIE, 1993.

[4] Strictly speaking, the photoelectron counts obtained from an ideal detector obey Poisson statistics with a variance equal to the mean photocount number. However, when the mean photocount is large, as is assumed here, the Gaussian distribution is an excellent approximation to the Poisson distribution.

[5] S. O. Rice, The mathematical analysis of random noise, Selected Papers on Noise and Stochastic Processes, N. Wax, Ed., Dover Pub. Co., New York, 1954

[6] Since the absolute detectable minimum signal strength levels have been mandated by the customer, of primary concern to receiver designers is, in the presence of turbulence, the minimum signal fluence that results in a $p_d = 95\%$ under various operational conditions. As a result, the primary application of the results derived here will be in the weak signal limit.

[7] V. I. Tatarski, The Effects of the Turbulent Atmosphere on Wave Propagation, Translated from Russian and issued by the National Technical Information Service, Dept. of Commerce, Springfield Va., 1971.

[8] Fried, D. L., *Scintillation of a ground-to-space laser illuminator*, J. Opt. Soc. Am., **57**, 980 - 983, (1967).

[9] Minott, P. O., *Scintillation in an earth-to-space propagation path*, J. Opt. Soc. Am., **62**, 885 - 888, (1972).

[10] R. F. Lutomirski, R. E. Huschke, W. C. Meecham, and H. T. Yura, *Degradations of laser systems by atmospheric turbulence*, Rand Corporation Report No. R-1171-ARPA/RC, June 1973.

[11]R. L. Mitchell, *Permanence of the log-normal distribution*, J. Opt. Soc. Am., **58**, 1267 - 1272 (1968).

[12]J. H. Churnside, *Aperture averaging of optical scintillations in the turbulent atmosphere*, Appl. Opt., **30**, 1982 - 1994 (1991).

[13]Although we are particularily interested here in ground-to-space propagation paths, we note that the present analysis is valid for arbitrary propagation paths (as long as $\sigma_{\ln I}^2 < 1$). For example, forhorizontal propagation through isotropic homogeneous turbulence, $\chi^2 \alpha \kappa^{7/6} C_n^2 L^{11/6}$, where L is the path length and $C_n^2$ is the index structure constant.

[14]*The Infrared and Electrooptical Systems Handbook*, Vol. 2, F. G. Smith, Ed., Chap. 2, Pub. by ERIM/SPIE, 1993.

[15] R. R. Beland, Phillips Laboratory, private communication.

[16]*The Infrared and Electrooptical Systems Handbook*, Vol. 2, F. G. Smith, Ed., Chap. 2, Pub. by ERIM/SPIE, 1993.

[17] R. R. Jones, J. W. Rockway, L. B. Stotts, D. W. Hanson, and A. J. Julian, *Submarine Laser Communications Evaluation Algorithm*, Naval Ocean Systems Center, Technical Report 672 (May 1981).

[18] Since daytime operational conditions are most stressing (e.g., high background noise), we employ daytime turbulence profiles here. In this regard, we note that a numerical fit to the nighttime experimental results at 0.488 μm reported in Ref. 6 is given by $\chi^2 \approx 0.02$ $\sec(Z)^{11/6}$, which is about a factor of 2.8 less than obtained from Eq. (3.7) for daytime conditions. However, if we employ the Navy-DARPA SLC nighttime model, where $\mu_{5/6} = 2.8 \times 10^{-10}$ $m^{7/6}$, we obtain that $\chi^2 = 0.013\ \lambda_{\mu m}^{-7/6} s(Z)^{11/6}$ ($\approx 0.03\ s(Z)^{11/6}$ at 0.488μm, in reasonable agreement with the experimental results given in Ref. 9).

## TECHNOLOGY OPERATIONS

The Aerospace Corporation functions as an "architect-engineer" for national security programs, specializing in advanced military space systems. The Corporation's Technology Operations supports the effective and timely development and operation of national security systems through scientific research and the application of advanced technology. Vital to the success of the Corporation is the technical staff's wide-ranging expertise and its ability to stay abreast of new technological developments and program support issues associated with rapidly evolving space systems. Contributing capabilities are provided by these individual Technology Centers:

**Electronics Technology Center:** Microelectronics, solid-state device physics, VLSI reliability, compound semiconductors, radiation hardening, data storage technologies, infrared detector devices and testing; electro-optics, quantum electronics, solid-state lasers, optical propagation and communications; cw and pulsed chemical laser development, optical resonators, beam control, atmospheric propagation, and laser effects and countermeasures; atomic frequency standards, applied laser spectroscopy, laser chemistry, laser optoelectronics, phase conjugation and coherent imaging, solar cell physics, battery electrochemistry, battery testing and evaluation.

**Mechanics and Materials Technology Center:** Evaluation and characterization of new materials: metals, alloys, ceramics, polymers and their composites, and new forms of carbon; development and analysis of thin films and deposition techniques; nondestructive evaluation, component failure analysis and reliability; fracture mechanics and stress corrosion; development and evaluation of hardened components; analysis and evaluation of materials at cryogenic and elevated temperatures; launch vehicle and reentry fluid mechanics, heat transfer and flight dynamics; chemical and electric propulsion; spacecraft structural mechanics, spacecraft survivability and vulnerability assessment; contamination, thermal and structural control; high temperature thermomechanics, gas kinetics and radiation; lubrication and surface phenomena.

**Space and Environment Technology Center:** Magnetospheric, auroral and cosmic ray physics, wave-particle interactions, magnetospheric plasma waves; atmospheric and ionospheric physics, density and composition of the upper atmosphere, remote sensing using atmospheric radiation; solar physics, infrared astronomy, infrared signature analysis; effects of solar activity, magnetic storms and nuclear explosions on the earth's atmosphere, ionosphere and magnetosphere; effects of electromagnetic and particulate radiations on space systems; space instrumentation; propellant chemistry, chemical dynamics, environmental chemistry, trace detection; atmospheric chemical reactions, atmospheric optics, light scattering, state-specific chemical reactions and radiative signatures of missile plumes, and sensor out-of-field-of-view rejection.